

LIST OF TABLES

Chapter II	Page No.
Table-II.1.	32
Heck coupling reaction in both water and in microemulsion media (water/Tween-20/Pn/Cy) as a function of [IL] in presence of TEA at a fixed ω ($= 30$) and 323K.	
Chapter III	
Table-III.1	48
Optimization of reaction condition for homocoupling reaction in RMs ^a	
Table-III.2	54
Homocoupling of different arylboronic acids ^a	
Table-III.3	56
Suzuki-Miyaura cross coupling of different Aryl halides with Phenylboronic acids	
Chapter IV	
Table-IV.1	73
Regioselectivity in product obtained from nitration reaction in IL/CTAB/1-octanol/decane microemulsion system.	
Chapter V	
Table-V.1	82
Interfacial, Thermodynamic and Interaction Parameters of Single and Mixed Surfactants.	

LIST OF SCHEMES

Chapter I	Page No.
Scheme-I.1	2
The two types of microemulsion: a) Direct microemulsion b) Inverse microemulsion	
Scheme-I 2	10
Ligand-free Suzuki reaction catalysed by Pd/C in microemulsion	
Scheme-I.3	11
The Heck Reaction in microemulsion media	
Scheme-I.4	11
Matsuda-Heck reaction between a p-methoxyphenyl diazonium salt and 2,3-dihydrofuran using a palladium catalyst	
Scheme-I.5	11
Sonogashira coupling reaction of iodobenzene with phenylacetylene in TX10 microemulsion	
Scheme-I.6	12
Sonogashira reaction catalysed by PdCl ₂ and NaOH in microemulsion	
Scheme-I.7	12
Hydrogenation of dimethyl itaconate formal reaction	
Scheme-I.8	13
The Diels Alder Reaction between <i>N</i> -ethylmaleimide and cyclopentadiene	
Scheme-I.9	13
The Diels Alder Reaction between <i>N</i> -ethylmaleimide and benzonitrile oxide	

Scheme-I.10	14
Dipolar benzonitrile oxide, in the innermost region of the microemulsion interface	
Scheme-I.11	14
The Diels alder Reaction in IL-microemulsion	
Scheme-I.12	15
Oxidation of cyclohexane with hydrogen peroxide	
Scheme I.13	15
Solvolysis of substituted benzoyl chloride	
Scheme-I.14	16
The condensation Reaction in o/w microemulsion	
Scheme-I.15	16
Aldol Condensation in acetone and p-nitrobenzaldehyde	
Scheme-I.16	17
Structures of prolinamide surfactants	
Scheme-I.17	17
Nitration of Phenol in O/W microemulsion with dilute Hydrochloric acid and sodium nitrate	
Scheme-I.18	18
Probable Mechanism for the Synthesis of 4-Chloro-2-(naphthalene-2-ylselanyl) Pyrimidine	
 Chapter II	
Scheme-II.1	22
Schematic representation showing possible interactions in microenvironment	
Scheme-II.2	31

Study of Heck reaction in microemulsion

Chapter III

Scheme-III.1 41

Molecular structure of AOT, DDAB, TX-100 and cyclohexane

Scheme-III.2 51

Homocoupling of arylboronic acid in RMs

Chapter IV

Scheme-IV.1 72

Pictorial representation of the nitration reaction in IL/CTAB/1-octanol/decane microemulsion system.

LIST OF FIGURES

Chapter I	Page No.
Figure-I.1	3
Pictorial representation of “phase diagram” of water, surfactant and oil mixtures.	
Chapter II	
Figure-II.1	23
Plots of $\Delta G_{o \rightarrow i}^0$ as a function of [IL] for water/Tween-20/Pn/Cy microemulsion system at ω (= 30) with varying temperatures. Inset A: Plots of interfacial composition (n_a^i/n_s) as a function of [IL] for water/Tween-20/ Pn/Cy microemulsion system at ω (= 30) with varying temperatures. Inset B: Same plots for K_d .	
Figure-II.2	26
Plots of $\Delta H_{o \rightarrow i}^0$ as a function of [IL] for water/Tween-20/Pn/Cy microemulsion system at ω (= 30) with varying temperatures. Inset A: Same plot for $\Delta S_{o \rightarrow i}^0$.	
Figure-III.3	33
The conductivity of microemulsion in absence and presence of IL (= 0.05 mol dm ⁻³) at regular interval during Heck reaction at 323K.	
Figure-IV.4	34
The variation of Gaussian profiles (area fraction) of the normalized spectra of different water species (bound water, bulk water) of IL containing (0.05 mol dm ⁻³) w/o microemulsion system with the reaction time.	
Chapter III	
Figure-III.1	42
The variation of electrical conductivity a function of water content (ω) for AOT (A), DDAB (B) and TX-100 (C) RMs, respectively in cyclohexane (Cy) at 303K.	

Figure-III.2

44

The variation of droplet size (A) and droplet count rate and (B) for AOT, DDAB and TX-100-Cy blended RMs as a function of water content (ω) at a fixed temperature (303K).

Figure-III.3

46

Representative normalized (normalized to intensity of 1.0) FTIR spectra of O-H band for AOT (A), DDAB (B) and TX-100 (C)- Cy blended RMs at a fixed water content ($\omega=5$) and temperature (303K). Specification: Experimental spectra (black curve), overall fitted line (red) and deconvoluted curves (bulk water (orange), bound water (green)).

Figure-III.4

46

The relative abundance [Gaussian profiles (area fraction)] of different water species (bulk (A) and bound (Bound)) in AOT, DDAB and TX-100–Cy blended RMs as a function of ω .

Figure-III.5

52

(A) The conductivity and (B) the hydrodynamic diameter (D_h) of RMs during course of the reaction.

Figure-III.6

53

The Gaussian Profiles of FTIR study of AOT RMs at regular interval during homocoupling reaction at fixed ω (= 15) and 303 K. Inset A. Representative normalized (normalized to intensity of 1.0) FTIR spectra of O-H band for blank AOT RMs at constant ω (= 15) and 303K. Specification: Experimental spectra (black curve), overall fitted points (red) and deconvoluted curves (1: bulk water; 2: bound water).

Chapter IV**Figure-IV.1**

65

(A) Plot of n_a/n_s vs. n_o/n_s at varied molar ratio of IL to surfactant (R); (B) Plots of ΔG_t^0 and interfacial composition (n_a^i/n_s) as a function of R for IL/CTAB/1-octanol/decane microemulsion system at fixed temperature of 358K.

Figure-IV.2 **66**

(A) Plots of ΔG_t^0 and (B) ΔH_t^0 (inset: ΔS_t^0) as a function of molar ratio of IL to surfactant for IL/CTAB/1-octanol/decane microemulsion system at four different temperatures (358→370 K).

Figure-IV.3 **69**

The pseudoternary phase diagram of IL/CTAB/1-octanol/decane microemulsion system at fixed surfactant-cosurfactant ratio (1:4, w/w) and temperature (358K).

Figure-IV.4 **71**

(A) Variation in the hydrodynamic diameter with the molar ratio of IL to surfactant (R) at two different temperatures (358 and 362 K), and (B) Variation of molecular interfacial area of the surfactant as a function of hydrodynamic diameter for IL/CTAB/1-octanol/decane microemulsion system.

Chapter V

Figure-V.1 **79**

Tensiometric (A) and Conductometric (B) determination of CMC of mixed aqueous CTAB/ $C_{16}E_{20}$ systems at equimolar composition at 303K.

Figure-V.2 **84**

(A) Measurement of zeta potential of single and binary (equimolar) surfactants in aqueous medium at 303K. (B) Hydrodynamic diameter (D_h) of micellar systems at 303 K. FESEM images of (C) CTAB/water and (D) CTAB/ $C_{16}E_{20}$ /water at micellar region, (E) CTAB/ $C_{16}E_{20}$ /water at post-micellar region, and (F) $C_{16}E_{20}$ /water at micellar region.

Figure-V.3 **85**

Optimized geometries at the B3LYP/6-31G level: (A) $C_{16}E_{20}/H_2O$ complex, (B) CTAB/ H_2O complex, and (C) CTAB/ $C_{16}E_{20}/H_2O$ complex. Colour code for atoms: blue, nitrogen; red, oxygen; dark gray, carbon; and light gray, hydrogen.

Figure-V.4 **86**

(A) Pictorial representation of Heck Reaction in self-organized media; and (B) Yield of Heck reaction in single (CTAB and $C_{16}E_{20}$) and mixed micelles (CTAB/ $C_{16}E_{20}$, 1:1) at 303K.

(A) Plot of n_a^i/n_s vs. water content (ω) for mixed CTAB/C₁₆E₂₀ microemulsions at equimolar composition comprising 0.5 mmol of mixed surfactant and 14.0 mmol of Hp or Dc stabilized by Pn. (B) Hydrodynamic diameter (D_h) as a function of ω for above mentioned systems. FESEM images of similar systems at a fixed $X_{C_{16}E_{20}} = 0.5$, $\omega = 10$ and 303 K, where (C) Hp and (D) Dc oils. (E) The variation of Gaussian profiles (area fraction) of the normalized spectra of different water species; and (F) Fluorescence lifetime of HCM $\langle\tau\rangle$ ($\lambda_{ex} = 310$ nm) as function of ω in CTAB/C₁₆E₂₀ (1:1)/Pn/Hp/water microemulsions at 303K.

Yield of Heck product (A) in individual constituents as well as in w/o mixed microemulsions (MEs), CTAB/C₁₆E₂₀ (1:1)/Pn/Hp or Dc/water at $\omega = 10$; and (B) variation of yield as a function of ω (= 10→50) in aforementioned MEs at 303K.

LIST OF PUBLICATION AND POSTER

Thesis Publication:

1. "Physicochemical studies of water-in-oil nonionic microemulsion in presence of benzimidazole-based ionic liquid and probing of microenvironment using model C-C cross coupling (Heck) reaction" **Barnali Kar**, Soumik Bardhan, Kaushik Kundu, Swapan Kumar Saha, Bidyut Kumar Paul, Sajal Das, RSC Advances, 2014, 4, 21000-21009.

2. "A fast and additive free C-C homo/cross-coupling reaction in reverse micellar galls: A brief understanding on role of surfactant, water content and base on the yield of product and possible reaction site therein" **Barnali Kar**, Soumik Bardhan, Prasanjit Ghosh, Bhaskar Ganguly, Kaushik Kundu, Sonali Sarkar, Bidyut Kumar Paul, Chemistry Select, 2017, 2, 1079-1088

3. "Synergistic Interaction of Surfactant Blends in Aqueous Medium Reciprocates in Non-polar Medium with Improved Efficacy as Nanoreactor" Soumik Bardhan, Kaushik Kundu, **Barnali Kar**, Gulmi Chakraborty, Dibbendu Ghosh, Debayan Sarkar, Sajal Das, Sanjib Senapati, Swapan Kumar Saha, Bidyut Kumar Paul, RSC Advances, 2016,6, 55104-55116

4. "Formation of High-Temperature Stable Benzimidazolium Ionic Liquid-in-Oil Microemulsion and Regioselective Nitration Reaction Therein" **Barnali Kar**, Soumik Bardhan, Kaushik Kundu, Prasanjit Ghosh, Bidyut Kumar Paul, Sajal Das, (Communicated)

Non-Thesis Publication:

1. "Microemulsion Mediated Organic Synthesis and the Possible Reaction Site" Prasanjit Ghosh, **Barnali Kar**, Soumik Bardhan, Kaushik Kundu, Swapan kumar Saha, Bidyut Kumar Paul, Sajal das, J. Surface Sci. Technol. 2016, 32, 8–16.

2. "The Mixing Behaviour of Anionic and Nonionic Surfactant Blends in Aqueous Environment Correlates in Fatty Acid Ester Medium" Kaushik Kundu, Arindam Das, Soumik Bardhan, Gulmi Chakraborty, Dibbendu Ghosh, **Barnali Kar**, Swapan K. Saha, Sanjib Senapati, Rajib Kumar Mitra, Bidyut K. Paul, Colloids and Surfaces A, 2016, 504, 331-342.

3. “Microemulsion (mEs) mediated rapid synthesis of Imidazo[1,2-a]pyridine and its late-stage functionalization” Prasanjit Ghosh, Bhaskar Ganguly, **Barnali Kar**, Sajal Das (Communicated)

4. “Microstructural Transition from Aqueous to Acetonitrile-based Non-aqueous Reverse Micelle: An Experimental and Theoretical Investigations” Madhurima Paul Chowdhury, Kaushik Kundu, Soumik Bardhan, **Barnali Kar**, Gulmi Chakraborty, Swapan Kumar Saha (Communicated)

Poster Presentation:

1. “Formation, thermodynamic properties and microstructures of water-in-oil nonionic microemulsion in presence of benzimidazole-based ionic liquid and probing of microenvironment via model C-C cross coupling (Heck) reaction” **Barnali Kar**, Soumik Bardhan, Kaushik Kundu, Swapan Kumar Saha, Bidyut K. Paul, Sajal Das, 5TH Asian Conference on Colloid and Interface Science, 2013, Department of Chemistry, University of North Bengal, Darjeeling.

2. “A fast and additive free Suzuki self/cross-coupling reaction in confined environment of reverse micellar galls” **Barnali Kar**, Soumik Bardhan, Bhaskar Ganguly, Sajal Das, National Symposium on RTPC-2015, 2015, Department of Chemistry, NIT Sikkim.

3. “Organic Reactions in Reverse Micelle” Barnali Kar, Soumik Bardhan, Bhaskar Ganguly, Prasanjit Ghosh, Sajal Das, 19TH CRSI National Symposium in Chemistry, 2016, Department of Chemistry, University of North Bengal, Darjeeling.

LIST OF APPENDICES

Appendix	Page No.
Appendix A	xvii-xxvi
Appendix B	xxvii
Appendix C	xxviii
Appendix D	xxix-xxxvi

Appendix A

Physicochemical studies of water-in-oil nonionic microemulsion in presence of benzimidazole-based ionic liquid and probing of microenvironment using model C-C cross coupling (Heck) reaction

[A] Basics of the dilution method and thermodynamics of the transfer of cosurfactant from oil to the interface

For a quaternary water-in-oil microemulsion system composed of water/ surfactant/cosurfactant /oil, the solubilization of water is governed by the distribution of cosurfactant molecules between oil and the interface at a fixed temperature. A small amount of cosurfactant may remain solubilized in the aqueous phase depending on its lipophilicity. A threshold amount of cosurfactant is required to stabilize a water-in-oil dispersion at a fixed molar ratio of water to surfactant (ω). As a result, an appropriate distribution constant (K_d) is attained, and governs cosurfactant molecules distributed between the interfacial region (consisting of surfactant molecules) and the oleic phase at a fixed temperature. The stable w/o microemulsion gets disrupted when excess oil is added and the system splits up into two distinct phases. Again, a threshold amount of cosurfactant is necessary to restore the w/o microemulsion equilibrium. This process is repeatedly followed in the dilution experiment. The concentrations of cosurfactant at the interface and in the bulk oil phase were estimated to get the distribution constant (K_d) by the dilution experiments in the light of the physicochemical rationale elaborated by Zheng et al.¹, Moulik et al.^{2,3}, Paul et al.⁴⁻⁶, and Abuin et al.⁷ The total number of moles of the cosurfactant, n_a present in the stable microemulsion is given by the relation,

$$n_a = n_a^i + n_a^w + n_a^o \quad (S1)$$

where, n_a^i , n_a^w , n_a^o are the number of moles of cosurfactant in the interfacial, water and oil phases respectively. Since the solubility of cosurfactant in the oil is constant at a given temperature, the constant k_o can be written as

$$k_o = \frac{n_a^o}{n_o} \quad (S2)$$

where n_o is the total number of moles of oil in the system. Combining Equations S1 and S2 we get

$$n_a = n_a^i + n_a^w + k_o n_o \quad (S3)$$

Since the moles of cosurfactant in the interface and in the dispersed phase (water) depend on the surfactant concentration, Equation S3 may be converted into a more convenient form by dividing throughout by total number of moles of surfactant, n_s to give

$$\frac{n_a}{n_s} = \frac{n_a^i + n_a^w}{n_s} + k_o \frac{n_o}{n_s} \quad (S4)$$

In our experiment, negligible water solubility of cosurfactant (P_n) leads to $n_a^w \approx 0$.⁵ Thus, above equation becomes,

$$\frac{n_a}{n_s} = \frac{n_a^i}{n_s} + k_o \frac{n_o}{n_s} \quad (S5)$$

A plot of n_a/n_s against n_o/n_s should yield the values of the slope (S) and the intercept (I). Slope (S) is actually k_o and n_a^o can be determined from Equation S2. On the other hand, n_a^i can be calculated from the intercept (I), which is equal to n_a^i/n_s .

The partition of Pn between the continuous oil phase and the interface of the droplet can be expressed in terms of the distribution constant (K_d). K_d can be calculated from the ratio of mole fraction of Pn in the interfacial composition (X_a^i) to the mole fraction of Pn in the bulk oil phase (X_a^o),

$$K_d = \frac{X_a^i}{X_a^o} = \frac{n_a^i/(n_a^i + n_s)}{n_a^o/(n_a^o + n_o)} = \frac{n_a^i(n_a^o + n_o)}{n_a^o(n_a^i + n_s)} \quad (S6)$$

Dividing numerator and denominator by $n_a^i n_a^o$, and putting the values of the slope (S) and the intercept (I) from Equation S5, we get

$$K_d = \frac{(1 + n_o/n_a^o)}{(1 + n_s/n_a^i)} = \frac{(1 + 1/S)}{(1 + 1/I)} = \frac{I(1 + S)}{S(1 + I)} \quad (S7)$$

The standard Gibbs free energy change of transfer (ΔG_{o-i}^0) of Pn from the continuous oil phase to the interfacial region, between the water and oil, is obtained from the relation

$$\Delta G_{o-i}^0 = -RT \ln K_d = -RT \ln \frac{X_a^i}{X_a^o} = -RT \ln \frac{I(1 + S)}{S(1 + I)} \quad (S8)$$

The Gibbs-Helmholtz equation⁸ was used to get the standard enthalpy of the said transfer process of alkanol from oil to interface (ΔH_{o-i}^0). Thus,

$$[\partial (\Delta G_{o-i}^0/T) / \partial T]_p = -\Delta H_{o-i}^0/T^2 \quad (S9)$$

Using chain rule of differentiation on the left hand side of equation (S9),

$$[\partial (\Delta G_{o-i}^0/T) / \partial T]_p = [\partial (\Delta G_{o-i}^0/T) / \partial (1/T)]_p [d(1/T)/dT] = [\partial (\Delta G_{o-i}^0/T) / \partial (1/T)]_p (-1/T^2) \quad (S10)$$

Substituting this value into eqn. S(9) we get,

$$[\partial (\Delta G_{o-i}^0/T) / \partial (1/T)]_p (-1/T^2) = -\Delta H_{o-i}^0/T^2 \quad (S11)$$

$$\text{Hence}^8, \Delta H_{o-i}^0 = [\partial (\Delta G_{o-i}^0/T) / \partial (1/T)]_p \quad (S12)$$

Herein, the $\Delta G_{o-i}^0/T$ vs. $1/T$ plots is nonlinear in nature in each case. Therefore, the points in $\Delta G_{o-i}^0/T$ vs. $1/T$ plots have been fitted in a 2^o polynomial equation as follows,

$$\Delta G_{o-i}^0/T = A + B (1/T) + C (1/T)^2 \quad (S13)$$

Where, A, B and C are the polynomial coefficients.

The first derivation of equation (S13) produced the enthalpy (ΔH_{o-i}^0),^{2,3}

$$\Delta H_{o-i}^0 = B + 2C^2 (1/T) \quad (S14)$$

Consequently, the corresponding entropy change (ΔS_{o-i}^0) can be found by the following relation,

$$\Delta S_{o-i}^0 = (\Delta H_{o-i}^0 - \Delta G_{o-i}^0)/T \quad (S15)$$

The evaluation of standard specific heat capacity change of transfer process, ($-\Delta C_p^0$)_{o-i}, follows from the relation,

$$[(\Delta C_p^0)]_{o-i} = [\partial \Delta H^0_{o-i} / \partial T]_p \quad (\text{S16})$$

The standard state herein considered is the hypothetical ideal state of the unit mole fraction.

[B] Interfacial composition of water (or, IL)/Tween-20/Pn/Cy microemulsion in absence and presence of IL

The dilution method was employed for a nonionic surfactant, Tween-20-based w/o microemulsion system stabilized in Pn (cosurfactant) and Cy (oil) with varying IL content (= 0.0, 0.05, 0.10, 0.15 and 0.20 mol dm⁻³) at a fixed ω (= 30) and temperatures (293K→323K). From the data collected, graphs were constructed by plotting n_a/n_s against n_o/n_s according to Eq. (S5). Representative plots are illustrated in Figure S1. The plots were strikingly linear (average correlation of coefficients was 0.9965). From the Figure S1, the values of n_a^o and n_a^i were obtained from slopes (S) and intercepts (I), respectively and subsequently all the thermodynamic parameters [K_d , ΔG^0_{o-i} , ΔH^0_{o-i} , ΔS^0_{o-i} and $(\Delta C_p^0)_{o-i}$] were evaluated according to Eqs. (S1-S16).²⁻⁶ The values of above physicochemical parameters are presented in Table S1.

In order to underline the influence of IL content on the interfacial composition of Tween-20-based w/o microemulsion systems stabilized in Pn and Cy under various physicochemical conditions (mentioned earlier), n_a^i/n_s values [i.e. compositional variations of amphiphiles (both Tween-20 and Pn) at the interface] are plotted against [IL] (0.0→0.20 mol dm⁻³) and respective plots are depicted in Figure 1 (inset A). It has been observed from Figure 1 (inset A) that n_a^i values gradually increase with increase in [IL] at all temperatures with some exceptions at low and high temperatures (293 and 323K). The increase in n_a^i values may be attributed to the salting out of the polar head group of Tween-20 in the aqueous phase (i.e., nano water pool), resulting in enhanced interfacial packing of Tween-20 and Pn. Small and polarizable anion (Br⁻) of 1-butyl-3-propyl benzimidazolium bromide tends to promote the water structure and dehydrate the ether oxygen of polyoxyethylene type nonionic surfactant (Tween-20 having 20 POE chains). Consequently, hydrophilicity of the surfactant (due to salting-out effect) decreases.⁹ Recently, it was reported that POE chains of Tween-20 produce electrostatic interaction with imidazolium cation, and thereby, stimulate the rigidity of IL/oil interface.^{10,11} Further, delocalization of the charge as well as the charge shielding due to the presence of both benzene and imidazolium ring in IL contribute the factor that influences the effective binding of Pn with IL and Tween-20 at the droplet surface. With increasing [IL], delocalization of charge will be more. Hence, requirement of Tween-20 molecules decreases at the interface, and consequently, Pn population (n_a^i) increases.¹² All these phenomena are responsible for observed increase in Pn population (n_a^i) at the interface with increase in [IL]. Similar results were also observed by Wang et al.¹³ for [bmim][BF₄]/Brij-35/1-butanol/toluene microemulsion with different m_{IL}/m_{H_2O} values at different temperatures. On the other hand, n_a^i increases with increase in temperature in absence and presence of IL with some exceptions at higher [IL]. It can be explained on the basis of the interactions between the active constituents at the interfacial layer of the microemulsion (for example, hydrogen bonding interaction between IL-water, dipole-dipole or dipole-induced dipole interaction between Pn-Tween-20, and ion-dipole interaction between IL-Pn and IL-Tween-20) (Scheme 1). With increase in temperature, all these interactions are diminished. Consequently, more Pn is accommodated at the interfacial layer, which imparts stability of the microemulsions.¹⁴ Similar behavior was also observed for both [C₁₂mim]Br/1-pentanol/octane/[bmim][BF₄] systems¹³ and CTAB/alkanol/toluene/[bmim][BF₄] systems.¹⁵ No systematic trend as a function of IL content has been observed for n_a^o values (Table S1) at the studied temperature range.

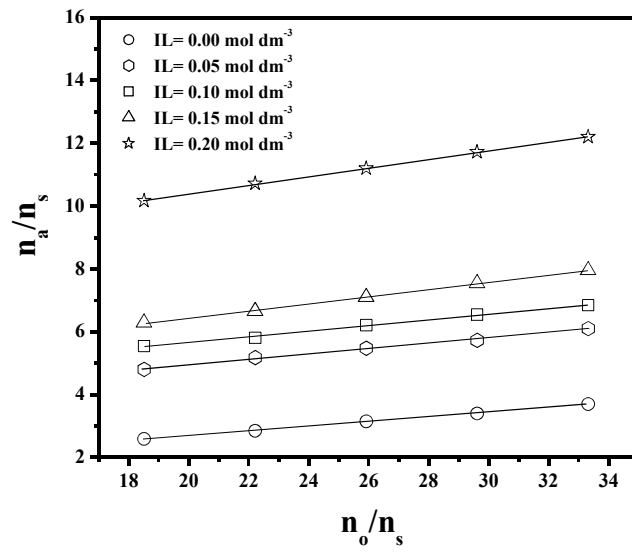


Figure-A.S1. Plots of n_a/n_s vs. n_o/n_s according to Eq. (S4) for water/Tween-20/ pentanol /cyclohexane microemulsion system with different [IL] at $\omega = 30$ at constant temperature of 303K.

Table-A.S1: Interfacial and bulk compositions of 1-pentanol, distribution constant (K_d) and thermodynamic parameters of its transfer from cyclohexane to the interface for w/o microemulsion containing 3.6 ml oil, 1 mmol of surfactant at constant ω ($= 30$) with varying [IL].

IL (mol dm ⁻³)	T(K)	$10^4 n_a^i$ (mol)	$10^3 n_a^o$ (mol)	K_d	$-\Delta G_{o \rightarrow i}^0$ (kJ mol ⁻¹)	$\Delta H_{o \rightarrow i}^0$ (kJ mol ⁻¹)	$\Delta S_{o \rightarrow i}^0$ (JK ⁻¹ mol ⁻¹)	$[\Delta C_p^0]_{o \rightarrow i}$ (kJ mol ⁻¹ K ⁻¹)
0.0	293	5.55	1.98	4.94	3.89	-32.58	-97.92	0.74
	303	5.82	1.23	7.81	5.18	-25.43	-66.83	
	313	9.34	1.25	9.35	5.82	-18.04	-39.03	
	323	9.99	1.00	11.79	6.63	-10.41	-11.69	
0.05	293	14.42	1.33	10.04	5.62	-11.70	-20.74	0.06
	303	16.18	1.41	9.76	5.74	-11.10	-17.69	
	313	16.46	1.00	13.57	6.79	-10.48	-11.80	
	323	17.10	1.07	13.94	6.86	-9.85	-9.25	
0.10	293	17.57	1.66	8.57	5.23	-14.15	-30.46	0.55
	303	18.95	1.57	9.21	5.59	-8.79	-10.56	
	313	18.03	1.07	13.01	6.68	-3.25	-10.97	
	323	18.12	1.15	12.7	6.70	2.48	28.42	
0.15	293	15.72	1.65	8.42	5.19	-4.07	3.82	-0.37
	303	20.8	1.90	7.88	5.20	-7.64	-8.07	
	313	22.28	1.23	11.85	6.43	-11.34	-15.69	
	323	17.75	1.15	12.09	6.69	-15.16	-26.21	
0.20	293	17.20	1.83	7.82	5.01	-0.4	15.73	-0.43
	303	39.55	2.16	7.72	5.15	-4.58	1.88	
	313	28.48	1.48	10.41	6.10	-8.89	-8.91	
	323	19.50	1.25	11.42	6.54	-13.34	-21.05	

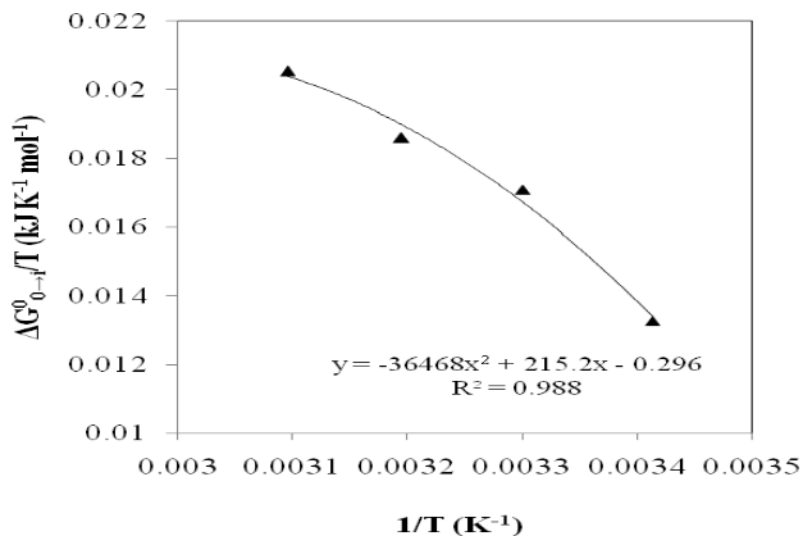


Figure-A.S2. Plots of nonlinear dependence of ($\Delta G_{o \rightarrow i}^0/T$) on ($1/T$) in terms of a two degree polynomial equation for water/Tween-20/pentanol/cyclohexane microemulsion system in absence of IL at $\omega = 30$ with varied temperature (293K \rightarrow 323K).

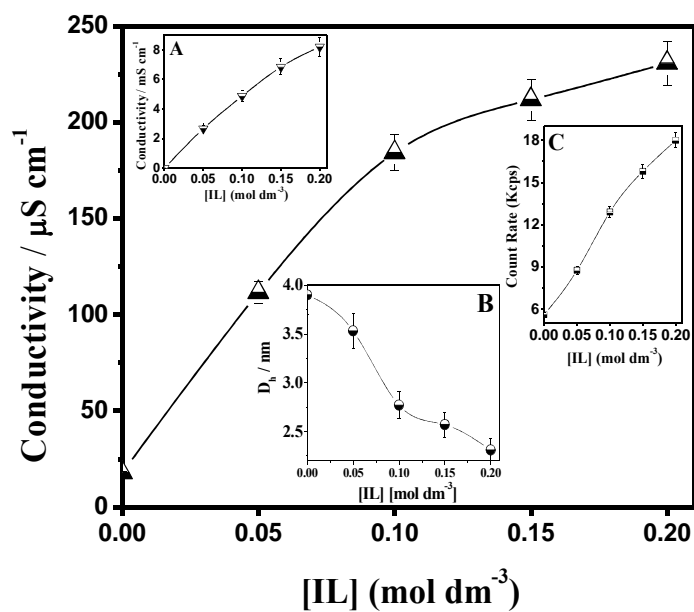


Figure-A.S3. A representative plot for the variation of conductance as a function of IL content for water/Tween-20 /pentanol/cyclohexane microemulsion system at $\omega (= 30)$ and 303K. Inset A: Result of blank experiment (same concentration of IL in water). Inset B and C: Hydrodynamic diameter (D_h) (B) and Count Rate (C) of the microemulsion droplets for the same w/o systems with increasing IL content at identical condition.

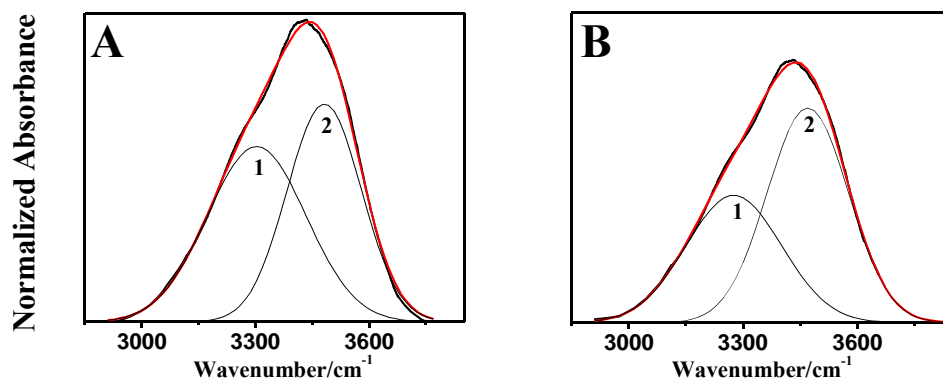


Figure-A.S4: Representative FTIR spectra of O-H band for water/Tween-20/pentanol/cyclohexane microemulsion system at constant ω ($= 30$) and fixed temperature (303K). (A) In absence of IL and (B) in presence of $[IL] = 0.20 \text{ mol dm}^{-3}$. Specification: Experimental spectra (black curve), overall fitted curve (red) and deconvoluted curves (1: bulk water; 2: bound water).

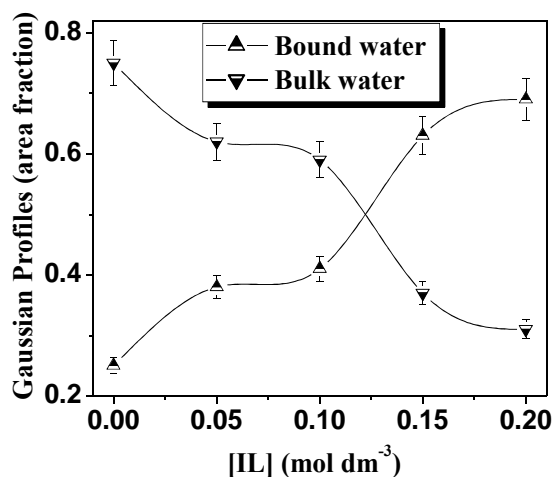
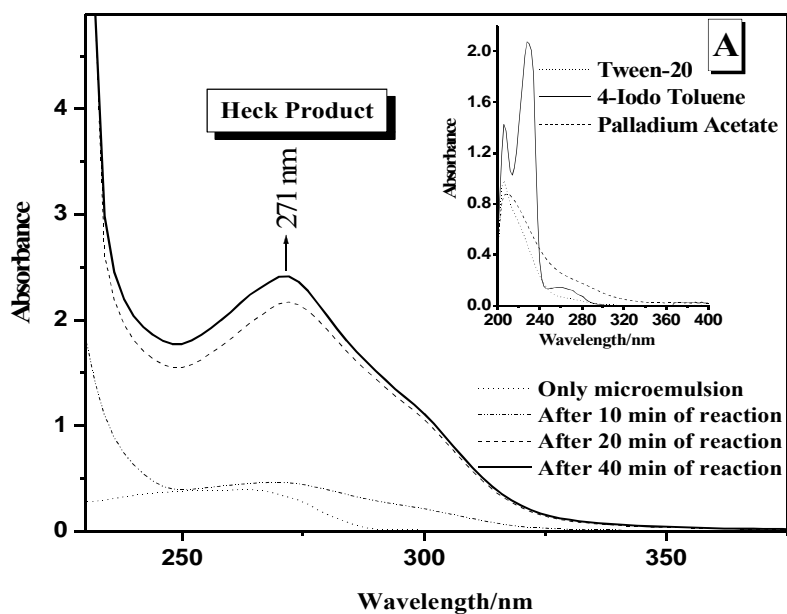
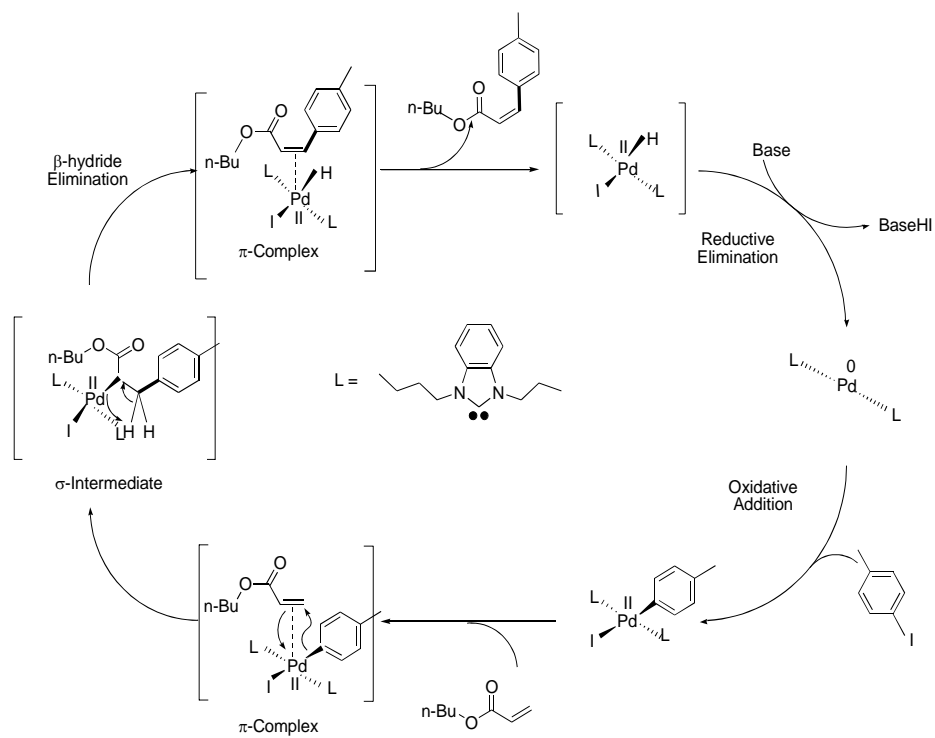


Figure-A.S5. The variation of Gaussian profiles (area fraction) of the normalized spectra of different water species in water/Tween-20/pentanol/cyclohexane as a function of IL content.

Table-A.S2. Heck coupling reaction in water (IL)/Tween-20/Pn/Cy microemulsion medium in presence of different bases at constant ω ($= 30$) and temperature (323K) ($[IL] = 0.05 \text{ mol dm}^{-3}$).

Entry	Base used	Time	Yield (%)
1	K ₂ CO ₃	1 hr.	30
2	NEt ₃	1 hr.	75
3	TMEDA	1 hr.	40



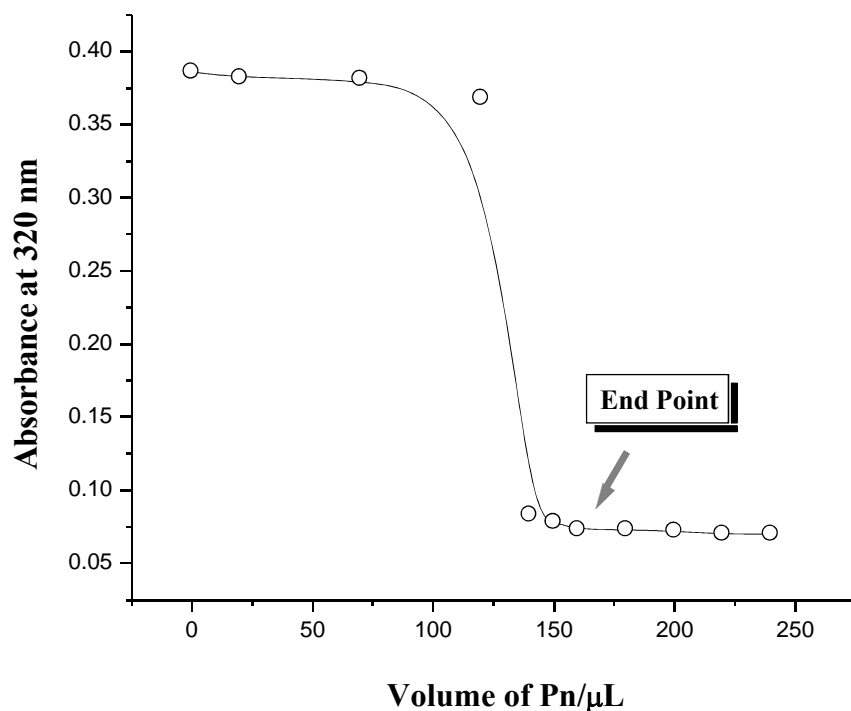


Figure-A.S7. Plots of sample absorbance (measured at 320 nm) vs. volume of pentanol (Pn) for water/Tween-20/pentanol/cyclohexane microemulsion system at $\omega = 30$ and constant temperature of 303K .

[C] Spectral analysis ($^1\text{H-NMR}$ and $^{13}\text{C-NMR}$)

1-Butyl-3-propylbenzimidazolium Bromide:

$^1\text{H-NMR}$ (CDCl_3 , 300 MHz) δ 1.01-0.92 (m, 6H), 1.42-1.32 (m, 2H), 2.02-1.87 (m, 4H), 4.40-4.33 (m, 4H), 7.61 (s, 1H), 7.64 (s, 1H), 10.30 (s, 1H); $^{13}\text{C-NMR}$ (CDCl_3 , 75 MHz) δ 11.5, 14.2, 20.2, 24.5, 32.9, 50.5, 52.1, 123.3, 123.4, 137.3.

4-methyl butyl cinnamate:

$^1\text{H-NMR}$ (CDCl_3 , 300MHz) δ 0.96 (t, 3H, $J = 7.2$ Hz), 1.44 (m, 2H), 1.68 (m, 2H), 2.36 (s, 3H), 4.20 (t, 2H, $J = 6.6$ Hz), 6.39 (d, 1H, $J = 16.2$ Hz), 7.18 (d, 2H, $J = 7.8$ Hz), 7.42 (d, 2H, $J = 7.8$ Hz), 7.66 (d, 2H, $J = 16.2$ Hz); $^{13}\text{C-NMR}$ (CDCl_3 , 75 MHz) δ 13.8, 19.2, 21.4, 30.8, 64.3, 117.2, 128.1, 129.6, 131.8, 140.6, 144.6, 167.3.

References:

1. O. Zheng, J-X. Zhao and X.-M. Fu, *Langmuir*, 2006, **22**, 3528-3532.

2. D. Mitra, I. Chakraborty, S.C. Bhattacharya, S.P. Moulik, S. Roy, D. Das and P.K. Das, *J. Phys.Chem. B*, 2006, **110**, 11314-11326.
3. K. Maiti, I. Chakraborty, S.C. Bhattacharya, A.K. Panda and S.P. Moulik, *J. Phys.Chem. B*, 2007, **111**, 14175-14185.
4. B.K. Paul and D.D. Nandy, *J. Colloid Interface Sci.*, 2007, **316**, 751-761.
5. K. Kundu, G. Guin and B. K. Paul, *J. Colloid Interface Sci.*, 2012, **385**, 96-110.
6. K. Kundu and B. K. Paul, *Colloid Polym. Sci.*, 2013, **291**, 613-632.
7. E. Abuin, E. Lissi and K. Olivares, *J. Colloid Interface Sci.*, 2004, **276**, 208-211.
8. Atkins' Physical Chemistry, P. Atkins, J. D. Paula, Oxford University Press, 2004, pp126.
9. R. K. Mitra and B. K. Paul, *J. Colloid and Interface Sci.*, 2005, **291**, 550-559.
10. S. Paul and A. K. Panda, *Colloids and Surfaces A: Physicochem. Eng. Aspects*, 2013, **419**, 113–124.
11. Y. Gao, L. Hilfert, A. Voigt and K. Sundmacher, *J. Phys. Chem. B*, 2008, **112**, 3711-3719.
12. S. Bardhan, K. Kundu, B. K. Paul and S. K. Saha, *Colloid Surfaces A*, 2013, **433**, 219-229. 13. F. Wang, Z. Zhang, D. Li, J. Yang, C. Chu and L. Xu, *J. Chem. Eng. Data*, 2011, **56**, 3328–3335.
14. J. Chai, L. Xu, W. Liu and M. Zhu, *J. Chem. Eng. Data*, 2012, **57**, 2394-2400.
15. Z. Zhang, F. Wang, D. Li and J. Yang, *J. Disp. Sci. Technol.*, 2012, **33**, 141-14

Appendix B

A fast and additive free C-C homo/cross-coupling reaction in reverse micellar gallsows: A brief understanding on role of surfactant, water content and base on the yield of product and possible reaction site therein

Table-B.S1. Basic Data of the electrical conductivity of AOT RMs at regular interval during homocoupling reaction at fixed ω (= 15) and temperature (303K).

Time	Conductivity/ $\mu\text{S cm}^{-1}$
Blank RM	0.15
Just adding Pd(OAc) ₂	0.18
5 min	0.16
Just adding reagent	0.19
2 min	0.19
4 min	0.22
6 min	0.24
8 min	0.26
10 min	0.279

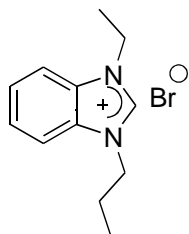
Table-B.S2. Basic data of DLS measurement of AOT RMs at regular interval during homocoupling reaction at fixed ω (= 15) and temperature (303K).

Time	D _n /nm
Blank RM	8.64 (±0.26)
Add reagent	13.35 (±0.40)
2 min	14.26 (±0.47)
4 min	15.90 (±0.43)
6 min	17.30 (±0.51)
8 min	19.33 (±0.59)
10 min	19.55 (±0.57)

Appendix C

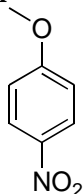
Formation of High-Temperature Stable Benzimidazolium Ionic Liquid-in-Oil Microemulsion and Regioselective Nitration Reaction Therein

1-Ethyl-3-Propyl Benzimidazolium Bromide



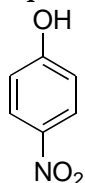
^1H NMR (CDCl_3 , 300 MHz) δ 0.96 (t, $J = 7.2$ Hz, 3H), 1.65 (t, $J = 7.2$ Hz, 3H), 4.54 (q, $J = 7.2$ Hz, 2H), 4.64 (q, $J = 7.2$ Hz, 2H), 7.29-7.63 (m, 2H), 7.71-7.79 (m, 2H). ^{13}C NMR (CDCl_3 , 75 MHz) δ

p-nitro anisole



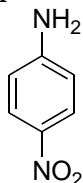
Yellow solid, MP = 52-54°C, ^1H NMR (CDCl_3 , 300 MHz) δ 3.90 (s, 3H), 6.93-6.99 (m, 2H), 8.17-8.23 (m, 2H), ^{13}C NMR (CDCl_3 , 75 MHz) δ 56.0, 114.0, 125.9, 141.5, 164.6.

p-nitro phenol



Yellow needles solid, MP = 113-115°C, ^1H NMR (CDCl_3 , 300 MHz) δ 6.86-6.91 (m, 2H), 8.03-8.08 (m, 2H), 11.01 (s, 1H), ^{13}C NMR (CDCl_3 , 75 MHz) δ 116.1, 126.5, 140.0, 164.3.

p-nitro aniline



Yellow needles solid, MP = 146-149°C, ^1H NMR (CDCl_3 , 300 MHz) δ 6.59-6.68 (m, 4H), 7.92-7.96 (m, 2H), ^{13}C NMR (CDCl_3 , 75 MHz) δ 112.8, 113.1, 126.8, 136.1, 156.1.

Appendix D

Synergistic Interaction of Surfactant Blends in Aqueous Medium Reciprocates in Non-polar Medium with Improved Efficacy as Nanoreactor

Analytical data for Heck Product (4-methyl butyl cinnamate):

$^1\text{H-NMR}$ (CDCl_3 , 300MHz) δ 0.96 (t, 3H, $J = 7.2$ Hz), 1.44 (m, 2H), 1.68 (m, 2H), 2.36 (s, 3H), 4.20 (t, 2H, $J = 6.6$ Hz), 6.39 (d, 1H, $J = 16.2$ Hz), 7.18 (d, 2H, $J = 7.8$ Hz), 7.42 (d, 2H, $J = 7.8$ Hz), 7.66 (d, 2H, $J = 16.2$ Hz); $^{13}\text{C-NMR}$ (CDCl_3 , 75 MHz) δ 13.8, 19.2, 21.5, 30.8, 64.4, 117.2, 128.0, 129.6, 131.7, 140.6, 144.6, 167.3.

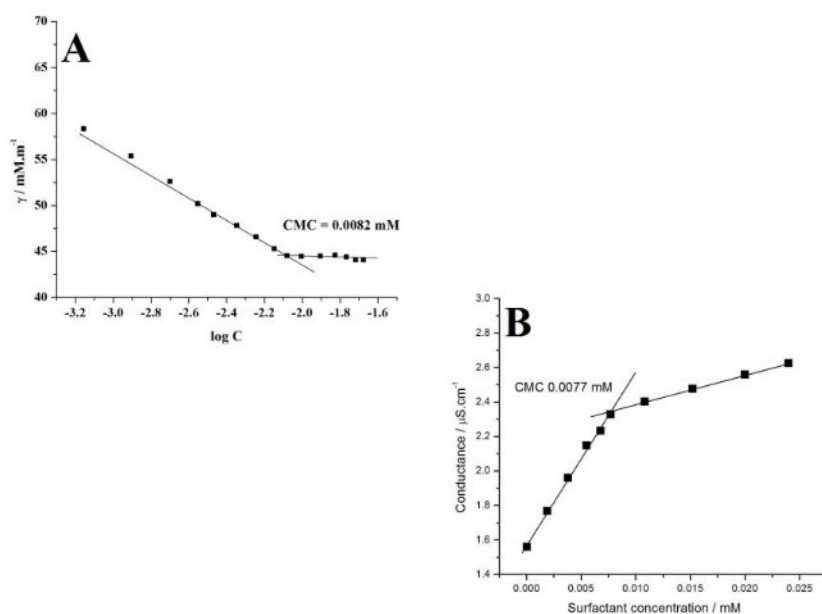


Figure-D.S1. Tensiometric (A) and conductometric (B) determination of critical micellar concentration (CMC) for single $\text{C}_{16}\text{E}_{20}$ surfactant system at a fixed temperature (303K).

Table-D.S1. Micellar parameters: experimental CMC values obtained from surface tension and conductivity techniques at 303K, literature CMC (CMC_{lit}) and ideal CMC (CMC_{ideal}) of binary mixture of cationic CTAB with non-ionic $C_{16}E_{20}$.

Micellar System	CMC_{exp} (mM)		CMC_{lit} (mM)	CMC_{ideal} (mM)
	Surface Tension	Conductance		
	CTAB	0.9301	-	0.92 ^a , 0.871 ^b
$C_{16}E_{20}$	0.0077	-	0.0080 ^c	-
CTAB/ $C_{16}E_{20}$ (1:1)	0.0105	0.0109	-	0.0150

^{a,c}Ref.¹ ^bRef.²



Figure-D.S2A. Optimized geometry at the B3LYP/6-31G level for isolated CTAB. Color code for atoms: blue, nitrogen; dark gray, carbon; and light gray, hydrogen

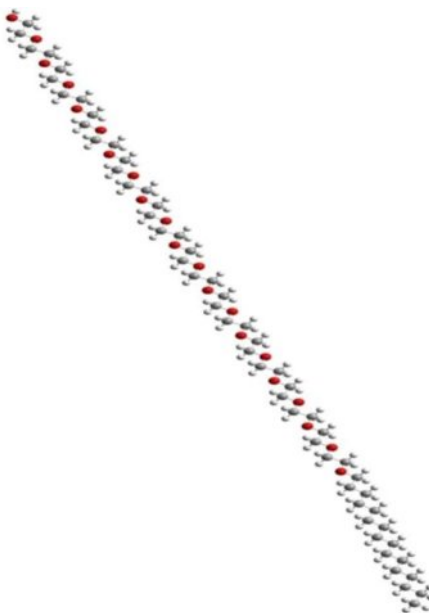


Figure-D.S2B. Optimized geometry at the B3LYP/6-31G level for isolated C₁₆E₂₀. Color code for atoms: red, oxygen; dark gray, carbon; and light gray, hydrogen

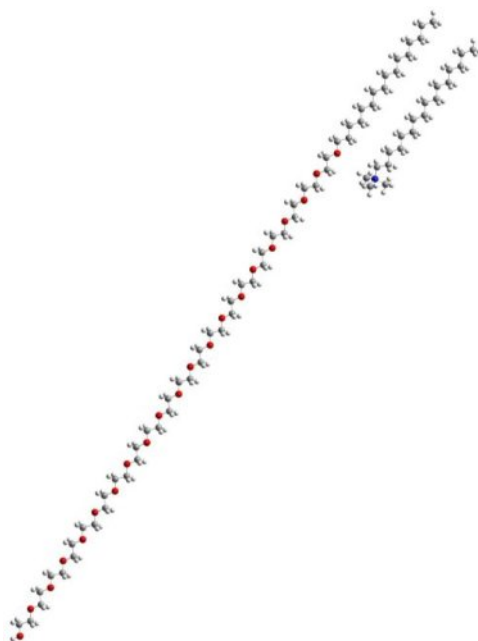


Figure-D.S2C. Optimized geometry at the B3LYP/6-31G level for CTAB/C₁₆E₂₀. Color code for atoms: blue, nitrogen; red, oxygen; dark gray, carbon; and light gray, hydrogen.

Table-D.S2. Optimization of C-C cross coupling Heck reaction in micelles and w/o mixed microemulsion media at 303K.^a

Entry	Solvent	Water content (ω)	Yield (%) ^d
1.	Water	-	07
2.	CTAB ^b	-	57
3.	C ₁₆ E ₂₀ ^b	-	44
4.	CTAB/ C ₁₆ E ₂₀ ^b	-	66
5.	Heptane (Hp)	-	37
6.	Decane (Dc)	-	15
7.	Hp/1-pentanol (Pn) (1:2, wt%)	-	40
8.	Dc/Pn (1:2, wt%)	-	19
9.	Water/CTAB/ C ₁₆ E ₂₀ /Pn/Hp ^c	10	79
10.	Water/CTAB/ C ₁₆ E ₂₀ /Pn/Hp ^c	20	70

11.	Water/CTAB/ C ₁₆ E ₂₀ /Pn/Hp ^c	30	59
12.	Water/CTAB/ C ₁₆ E ₂₀ /Pn/Hp ^c	40	56
13.	Water/CTAB/ C ₁₆ E ₂₀ /Pn/Hp ^c	50	54
14.	Water/CTAB/ C ₁₆ E ₂₀ /Pn/Dc ^c	10	68
15.	Water/CTAB/ C ₁₆ E ₂₀ /Pn/Dc ^c	20	57
16.	Water/CTAB/ C ₁₆ E ₂₀ /Pn/Dc ^c	30	45
17.	Water/CTAB/ C ₁₆ E ₂₀ /Pn/Dc ^c	40	44
18.	Water/CTAB/ C ₁₆ E ₂₀ /Pn/Dc ^c	50	41

^a Reaction condition: 4-iodo toluene (0.5 mmol), n-butyl acrylate (0.6 mmol), Triethylamine (1.0 mmol), Pd(OAc)₂ (0.02 mmol, 4 mol%), temperature; 303K, ^b Micellar system, [CTAB]= 0.9301 mM, [C₁₆E₂₀] = 0.0077 mM, [CTAB]:[C₁₆E₂₀] (1:1) = 0.0105 mM, ^c w/o mixed microemulsion; [water/CTAB/C₁₆E₂₀/Pn/oil, [CTAB]:[C₁₆E₂₀] (1:1); S:CS = 1:2 wt.%], ^d HPLC yield of the Heck product.

Table-D.S3. Interfacial composition and thermodynamic parameters of CTAB/C₁₆E₂₀/1-pentanol/*n*-heptane (or *n*-decane)/water microemulsion at 303K with varying water content (ω).

Ω	10	20	30	40	50
$10^4 n_a^i/\text{mol}$	15.30 (10.12) ^c	9.90 (7.42)	7.39 (5.92)	6.60 (5.45)	5.69 (4.68)
$10^4 n_a^0/\text{mol}$	10.29 (23.29)	20.59 (26.73)	28.50 (31.75)	33.34 (37.67)	42.48 (49.96)
K_d	20.65 (13.25)	10.46 (8.77)	5.24 (5.03)	4.07 (3.86)	3.54 (3.26)
$-\Delta G_t^0/\text{KJ mol}^{-1}$	7.62 (6.50)	5.91 (5.47)	4.17 (4.07)	3.53 (3.40)	3.18 (2.98)

^aAll the mixed microemulsion systems are formed using constant amount of mixed surfactant (0.5 mmol) and oil (14.0 mmol).

^bThe average errors in K_d and ΔG_t^0 were within ± 5 and $\pm 3\%$, respectively.

^cThe values in parentheses indicate parameters for *n*-decane (Dc) stabilized system.

Evaluation of interfacial and bulk composition of cosurfactant from thermodynamic point of view by the dilution method

W/o microemulsion consists of dispersion of water droplets in Hp or Dc continuum wherein the mixed surfactants (CTAB and C₁₆E₂₀ at equimolar composition) were considered to populate at the oil/water interface in partial association with the cosurfactant (Pn), which remained distributed between the

interface and the bulk oil, because of its negligible solubility in water.³ Thus, at a fixed [surfactant(s)], a critical concentration of Pn is required for the stabilization of the mixed microemulsions. Addition of extra oil (Hp or Dc) extracts Pn from the interface to destabilize the system, which can be stabilized by the addition of extra cosurfactant in the system. This is the fundamental basis of oil dilution experiment (the dilution method). The following equations are helpful to rationalize the distribution vis-à-vis transfer process of Pn from the continuous oil phase to the interfacial region:

$$k_o = n_a^o/n_o \quad (S1)$$

$$\frac{n_a}{n_s} = \frac{n_a^i}{n_s} + k_o \frac{n_o}{n_s} \quad (S2)$$

$$K_d = X_a^i/X_a^o = \frac{n_a^i/n_a^i+n_s}{n_a^o/n_a^o+n_o} = \frac{n_a^i(n_a^o+n_o)}{n_a^o(n_a^i+n_s)} \quad (S3)$$

$$\Delta G_t^0 = -RT \ln K_d = -RT \ln \frac{X_a^i}{X_a^o} = -RT \ln \frac{I(1+S)}{S(1+I)} \quad (S4)$$

where, n_a , (n_a^i) and Gibbs free energy ($-\Delta G_t^0$), n_a^o , n_o , n_s denote the total number of moles of cosurfactant, its number at the interface, in the oil phase, the total number of moles of oil and the total number of moles of surfactant, respectively. A plot of n_a/n_s against n_o/n_s (Fig. S3) according to Eq. (S2) yields the values of the slope (S) and the intercept (I). Slope (S) is actually k_o and n_a^o can be determined from Eq. (S1). On the other hand, n_a^i can be calculated from the intercept (I), which is equal to n_a^i/n_s . The partition of cosurfactant between the continuous oil phase and the interface of the droplet can be expressed in terms of the distribution constant, which is represented by K_d . X_a^i and X_a^o are the mole fraction of alkanol in the interfacial layer and in the oil, respectively. ΔG_t^0 represents standard Gibbs free energy change of transfer of cosurfactant from oil to the interface.

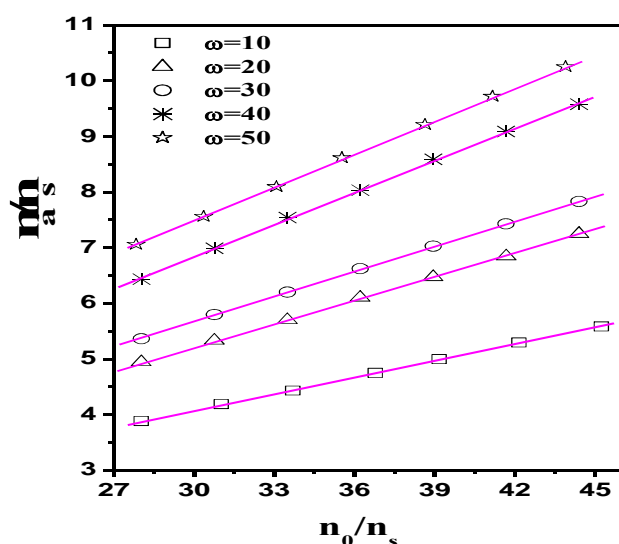


Figure-D.S3. Plot of n_a/n_s against n_o/n_s for systems comprising equimolar (1:1) mixed surfactant (CTAB and $C_{16}E_{20}$) (0.5mmol) and n-decane (14.0 mmol) stabilized by 1-Pn with different ω (10→50) at a constant temperature (303K).

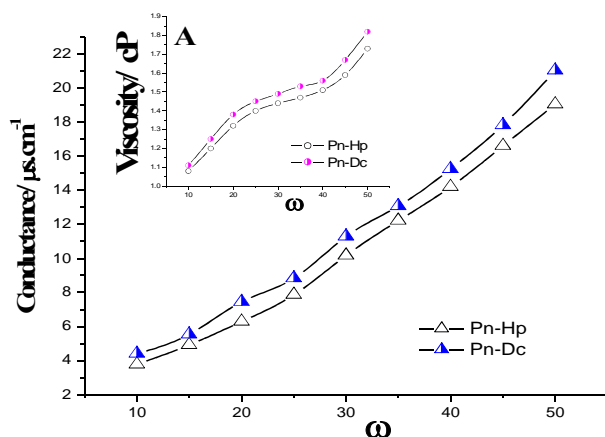


Figure-D.S4. Dependence of conductance value on water content (ω) for CTAB/ $C_{16}E_{20}$ (1:1)/Pn/Hp (Dc)/water microemulsions at 303K. **Inset A:** Dependence of viscosity on water content (ω) for the same systems of similar composition at 303K.

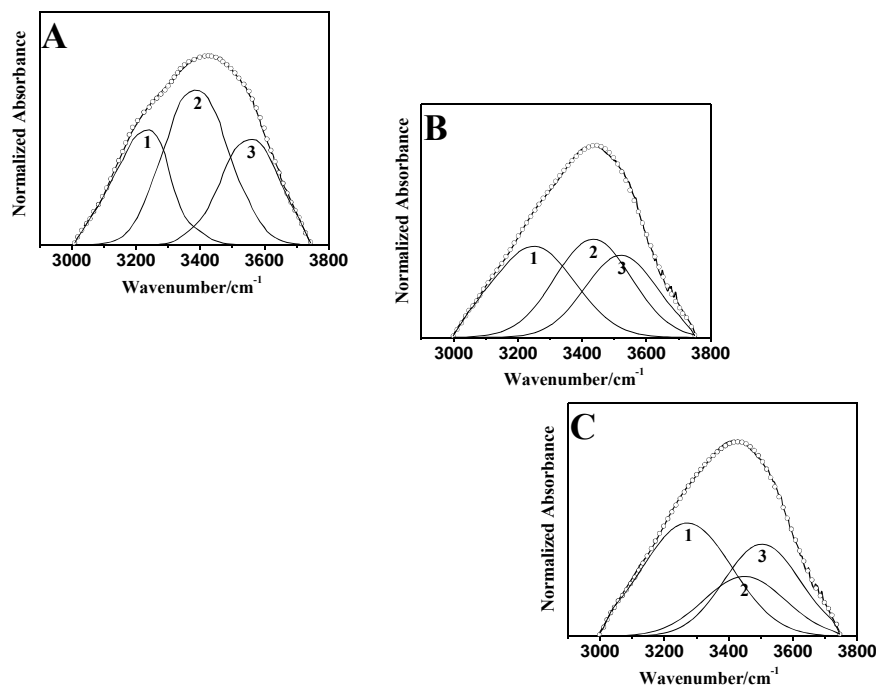


Figure-D.S5. Representative FTIR spectra of O-H band for w/o mixed surfactant microemulsions, CTAB/ $C_{16}E_{20}$ /Pn/Hp/water at equimolar composition (1:1) as a function water content (ω) at fixed **surfactant and cosurfactant mass ratio (1:2)** and temperature (303K) [A: $\omega = 10$; B: $\omega = 30$; and, C: $\omega = 50$ (Specification: experimental spectra, overall fitted curve (open circle) and deconvoluted curves (1: free water; 2: bound water; 3: trapped water)].

Reference:

- 1] S.K.Mehta, S. Chaudhary, *Colloids Surf. B* 2011, **83**, 139-147.
- 2] T.Chakraborty, S. Ghosh, S.P.Moulik, *J. Phys. Chem. B* 2005, **109**, 14813-14823.
- 3] S.P.Moulik, L.G.Digout, W.M.Aylward, R. Palepu, *Langmuir*, 2000, **16**, 3101-3106.